Peterhead CCS Project

Doc Title: Petrophysical Modelling Report

Doc No.: **PCCS-05-PT-ZP-9032-00001**
Date of issue: **19/03/2015**
Revision: **K03**
DECC Ref No: **11.111**
Knowledge Cat: **KKD - Subsurface**

KEYWORDS

Goldeneye, CO_2, porosity, net to gross, saturation, logs, capillary, contacts.

Produced by Shell U.K. Limited

ECCN: EAR 99 Deminimus

IMPORTANT NOTICE

Information provided further to UK CCS Commercialisation Programme (the **Competition**)

The information set out herein (the **Information**) has been prepared by Shell U.K. Limited and its sub-contractors (the **Consortium**) solely for the Department for Energy and Climate Change in connection with the Competition. The Information does not amount to advice on CCS technology or any CCS engineering, commercial, financial, regulatory, legal or other solutions on which any reliance should be placed. Accordingly, no member of the Consortium makes (and the UK Government does not make) any representation, warranty or undertaking, express or implied as to the accuracy, adequacy or completeness of any of the Information and no reliance may be placed on the Information. In so far as permitted by law, no member of the Consortium or any company in the same group as any member of the Consortium or their respective officers, employees or agents accepts (and the UK Government does not accept) any responsibility or liability of any kind, whether for negligence or any other reason, for any damage or loss arising from any use of or any reliance placed on the Information or any subsequent communication of the Information. Each person to whom the Information is made available must make their own independent assessment of the Information after making such investigation and taking professional technical, engineering, commercial, regulatory, financial, legal or other advice, as they deem necessary.

Table of Contents

Table of Figures

List of Tables

Executive Summary

This report covers the petrophysical input, methods and interpretation results for the provision of reservoir properties and fluid contacts for the Goldeneye field, its overburden and the contiguous aquifer in the context of the Peterhead Carbon Capture and Storage (CCS) project. The results of the work are used to populate both static and dynamic model suites which provide volumetrics and understanding of fluid behaviour. They are additionally used to support geomechanical modelling which provides understanding of the impact of changes in pressure and stress on the area. The report is an update of the previously-released petrophysical evaluation report for the Longannet CCS project to incorporate material on grain and fluid density estimation and on stress corrections, along with minor changes for clarity and grammar.

The evaluation is primarily based on datasets which were acquired from the five exploration and development wells in and immediately adjacent to the Goldeneye field, the location where routine and special core data are mainly concentrated. For the aquifer model the scope of interpretation is extended to cover a wider area, including surrounding fields such as Atlantic, Hannay, Hoylake, and Cromarty. In total, 26 wells were assessed. An initial quality control step on the raw logs was followed by stepwise derivation of shale volume (Vsh), net/gross, porosity, permeability and hydrocarbon saturation. Pressure data was additionally employed to allow the estimation of fluid contacts. Special core analysis data was used to help derive a saturation-height function for dynamic modelling.

Key deliverables are porosity, permeability, net to gross, fluid contacts and hydrocarbon saturations as digital files per well, and the saturation height model for the full field dynamic model. Porosity, permeability, net to gross and chalk capillary entry pressures were similarly provided for the overburden, aquifer and geomechanical models. For these latter models, it was necessary to use analogue data to represent some properties, primarily permeability and capillary entry pressure, because of limited data acquisition in Goldeneye overburden formations and in the Captain fairway sands near the Goldeneye field.

1. Introduction

The Peterhead CCS Project aims to capture around one million tonnes of CO_2 per annum, over a period of 10 to 15 years, from an existing combined cycle gas turbine (CCGT) located at SSE's Peterhead Power Station in Aberdeenshire, Scotland. This would be the world's first commercial scale demonstration of CO_2 capture, transport and offshore geological storage from a (post combustion) gas-fired power station.

Post cessation of production, the Goldeneye gas-condensate production facility will be modified to allow the injection of dense phase CO_2 captured from the post-combustion gases of Peterhead Power Station into the depleted Goldeneye reservoir.

The CO_2 will be captured from the flue gas produced by one of the gas turbines at Peterhead Power Station (GT-13) using amine based technology provided by CanSolv (a wholly owned subsidiary of Shell). After capture the CO_2 will be routed to a compression facility, where it will be compressed, cooled and conditioned for water and oxygen removal to meet suitable transportation and storage specifications. The resulting dense phase CO_2 stream will be transported direct offshore to the wellhead platform via a new offshore pipeline which will tie-in subsea to the existing Goldeneye pipeline.

Once at the platform the CO_2 will be injected into the Goldeneye CO_2 Store (a depleted hydrocarbon gas reservoir), more than 2 km under the seabed of the North Sea. The project layout is depicted in Figure 1-1 below:

Figure 1-1: Project Location

1.1. Summary

This document compiles the petrophysical input, methods and interpretation results, which were used to populate the reservoir properties in the Goldeneye static and dynamic models for full field, overburden and aquifer. The comprehensive evaluation is based on datasets which were acquired from exploration and development wells in the Goldeneye field, the location where routine and special core data are mainly concentrated. For the aquifer model the scope of interpretation is extended to cover a wider area, including surrounding fields such as Atlantic, Hannay, Hoylake, and Cromarty. Key deliverables are porosity, permeability, net to gross, fluid contacts and the saturation height model for the full field model (FFM), and porosity, permeability, net to gross and chalk capillary entry pressure for overburden and aquifer models. For these latter models, it was necessary to use analogue data to represent the properties, primarily permeability and capillary entry pressure, because of limited data acquisition in Goldeneye overburden formations and in the Captain fairway sands near the Goldeneye field.

2. Data Availability and Quality Control

Well data availability, data type and contribution are listed in Table 2-1.

Table 2-1: Well Input Data Summary

Well	Year	Wireline/LWD	Routine Core	SCAL	RFT/MDT	Image data	Drilling fluid	Input to Model
In & near-field Exploration								
14/29a-2 (near-field)	1980	Y	N (MCT*)	N	Y	N	WBM	FFM, overburden
14/29a-3	1996	Y	Y	Y	Y	Y	OBM	FFM, overburden, aquifer
14/29a-5	1999	Y	Y	Limited	Y	Y	OBM	FFM, overburden, aquifer
20/4b-6	1998	Y	Y	Y	Y	Y	WBM	FFM, overburden, aquifer
20/4b-7	2000	Y	Y	N	Y	Y	OBM	FFM, overburden, aquifer
Production wells (logged pre-production)								
GYA01	2004	Limited	N	N	N	N	OBM	Trajectory
GYA02	2004	Limited	N	N	N	N	OBM	Trajectory
GYA03	2004	Limited	N	N	N	N	OBM	Trajectory
GYA04	2004	Limited	N	N	N	N	OBM	Trajectory
GYA05	2004	Limited	N	N	N	N	OBM	Trajectory

Well	Year	Wireline/LWD	Routine Core	SCAL	RFT/MDT	Image data	Drilling fluid	Input to Model
Captain Fairway wells								
13/30-1	1981	Y	N	N	Y	N	WBM	Aquifer
13/30-2	1984	Y	N	N	Y	N	WBM	Aquifer
13/30-3	1986	Y	N	N	Y	N	OBM	Aquifer
13/30a-4	1998	Y	N	N	Y	N	WBM	Aquifer
14/26-1	1988	Y	N	N	Y	N	WBM	Aquifer
14/26a-6	1997	Y	Y	N	N	N	WBM	Aquifer
14/26a-7a	1999	Y	Y	N	Y	N	OBM	Aquifer
14/26a-8	2000	Y	N	N	N	N	OBM	Aquifer
14/28b-2	1997	Y	Y	N	Y	N	WBM	Aquifer
14/29a-4	1998	Y	Y	N	Y	Y	WBM	Aquifer
14/30b-3	1991	Y	N	N	N	N	OBM	Overburden Aquifer
20/4b-3	1989	Y	N	N	Y	N	OBM	Aquifer
20/5c-6	1997	Y	Y		Y	N	WBM	Aquifer
13/24-1	1974	Y	N	N	N	N	WBM	Overburden
14/28a-1	1990	Y	N	N	N	N	WBM	Overburden
20/1-1	1979	Y	N	N	N	N	WBM	Overburden

Notes: *MCT = Mechanical Coring Tool.

Borehole imaging logs only used for geomechanics

The in-field wells and the near-field Exploration well are shown on the field top structure map of Figure 2-1. The other wells from the Captain fairway are shown in Figure 2-2.

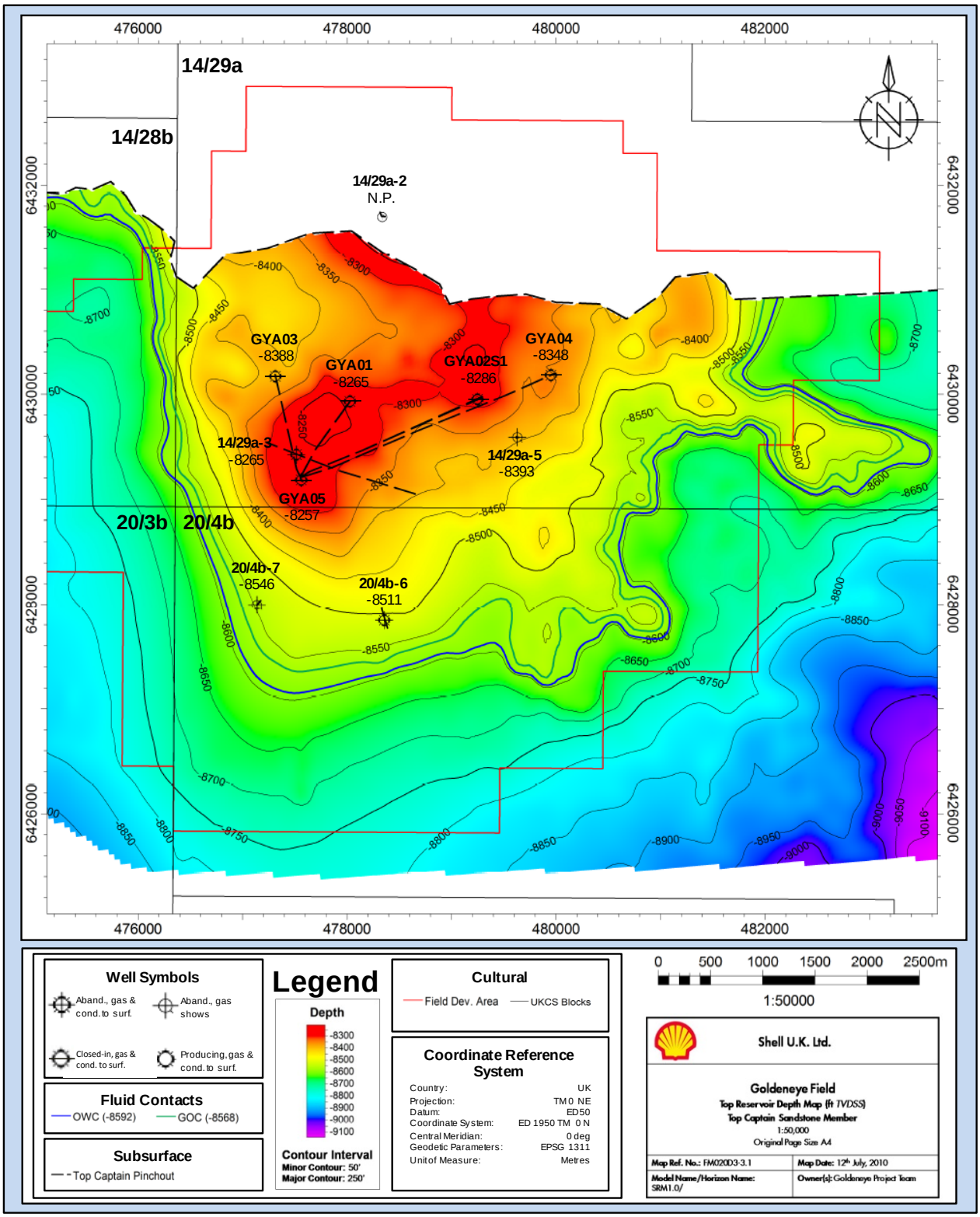

Figure 2-1: Map of Goldeneye field at top Captain level showing well locations

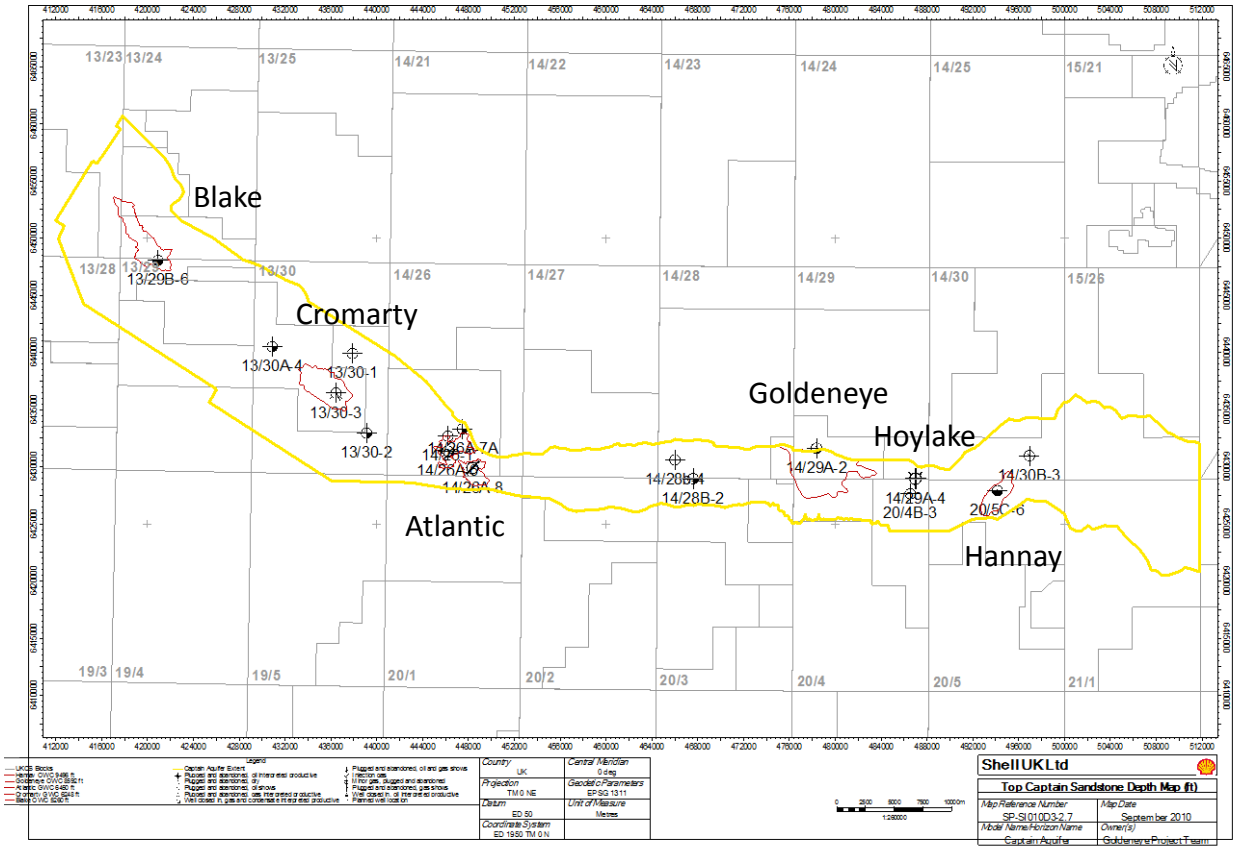

Figure 2-2: Captain fairway wells used in this report

2.1. Quality Control

For the Static Reservoir Model (Key Knowledge Deliverable 11.108 (1)), each Goldeneye well was evaluated individually to ensure that the effects of different logging tools and backgrounds were addressed properly. Environmental corrections were performed on bulk density and neutron porosity to correct for hole-size effect. There is no need for other neutron corrections because porosity is calculated solely from bulk density. The resistivity curve is borehole size corrected in all Goldeneye exploration & development wells and invasion corrected in 20/4b-6 where water-based mud (WBM) was used.

For the overburden and aquifer models gamma ray (GR) normalization was performed to generate shale volume consistency for the net to gross calculation. The resulting distribution in the Captain sandstones is relatively uniform (Figure 2-3), sharing a similar data density distribution profile. The GR-based shale volume is chosen over neutron–density (N-D) due to missing bulk density data in the older wells.

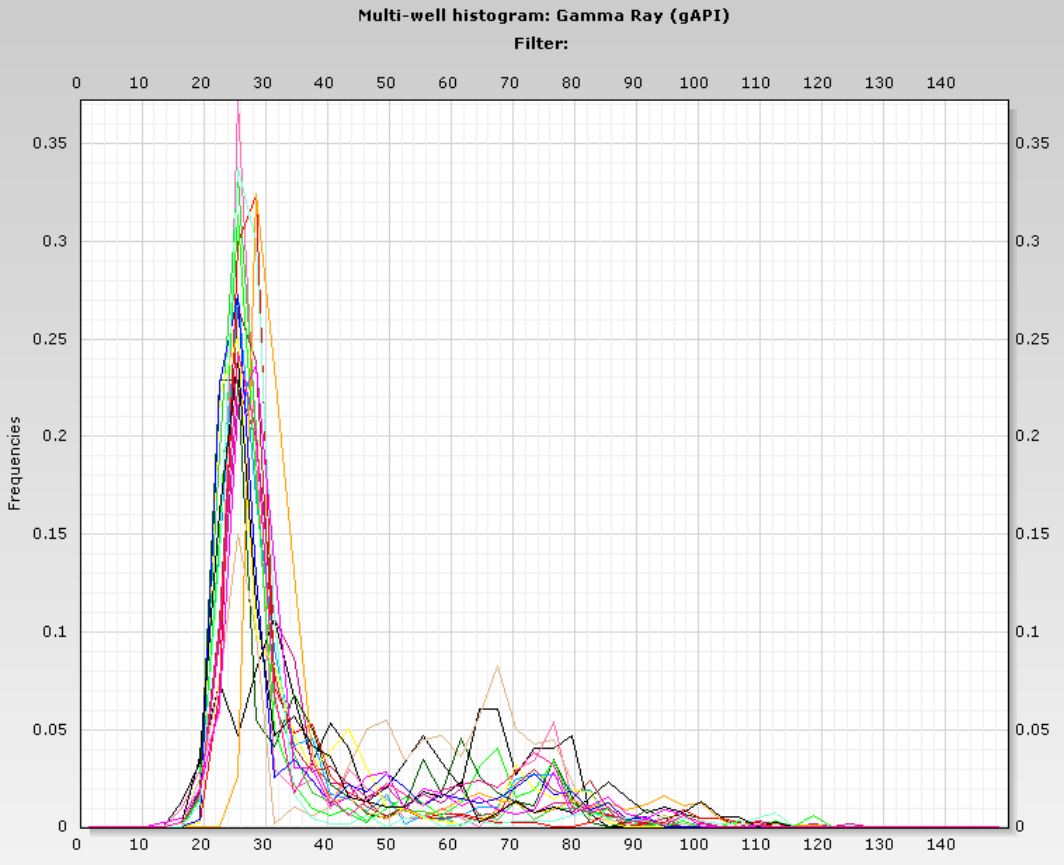

Figure 2-3: **Normalised GR distribution profile in Captain sandstone of Goldeneye & surrounding wells (16 wells).**

2.2. Formation Tops

Formation tops are exported from the static models where they had been selected according to sedimentary and structural characters from core, cuttings and logs. A full zonation list is given in Table 2-2. The Rødby formation is the primary seal for the Captain sandstone, and the Captain sandstone is zoned into subunits.

Table 2-2: **Goldeneye stratigraphy, overburden to Captain sandstone and underburden**

Group	Member/Units
Nordland	
Westray	Skade Fm
	Lark Fm
Stronsay	Mousa Fm
Moray	Beauly Mb
	Upper Dornoch Sst
	Dornoch Mudstone Unit
	Lower Dornoch Sst
Montrose	Lista Fm
	Mey Sst

	Upper Balmoral Sst
	Upper Balmoral and Tuffite Sst
	Maureen Fm
Chalk	Ekofisk Fm
	Tor Fm
	Hod Fm
	Herring Fm
	Plenus Marl Fm
	Hidra Fm
Cromer Knoll	Rødby Fm
	Valhall / Upper Valhall Mb
	Kopervik Sst
	Captain Sst subunit E
	Captain Sst subunit D
	Captain Sst subunit C
	Captain Sst subunit A
	Lower Valhall Mb
Humber	Kimmeridge Clay Fm
	Burns Sandstone

Note: There is no Captain B subunit

2.3. Petrophysical Facies

Sand quality and clean sand thickness control petrophysical facies which can be expressed in three classes based on core description (grain size, depositional environment) and logging response. The classes were assigned manually and are:

- **Class 1**

  Massive or substantially thick and clean sandstones are seen in the Captain A and D subunits. It exists occasionally within subunit C (e.g. in 14/29a-3). Sand thickness in this class is 25 ft [8 m] or more and has uniform medium grain size.

- **Class 2**

  The uppermost interval of the Captain sands is slightly muddy, containing 2 to 3% clay fraction in some locations, possibly representing injection from massive sandstone subunits. It makes up the bulk of subunit E.

- **Class 3**

  Heterogeneous clastic sequences with varying sand quality and mudstone content. It typically exists in subunit C which has a large number of thin sandstone layers.

The facies distribution is shown in Figure 2-4 and listed in Appendix 1. Permeability facies-class depths, Table 6-3.

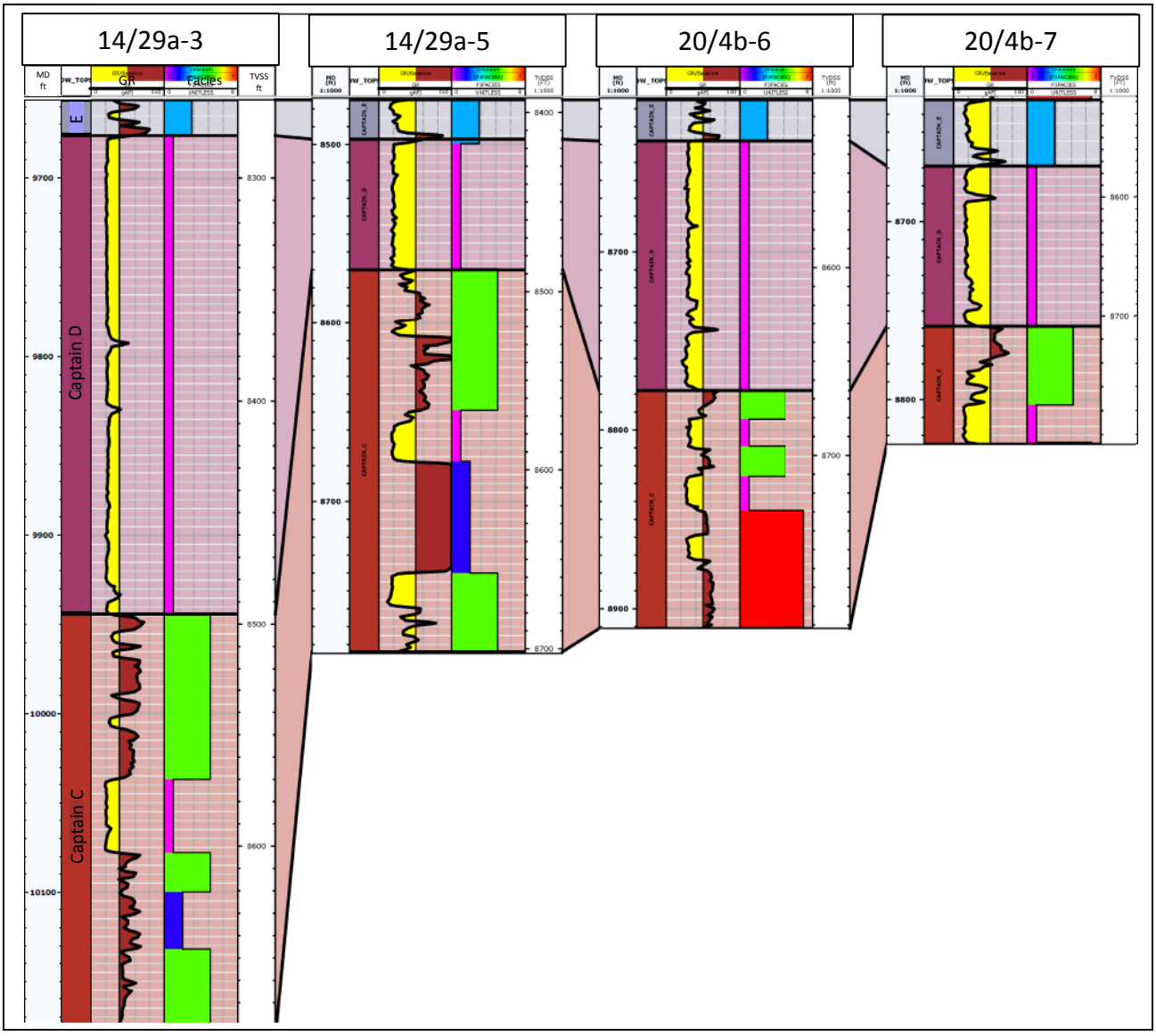

Figure 2-4: Petrophysical facies distribution in Goldeneye Exploration wells

Note: Class 1: Purple. Class 2: light blue. Class 3: green. Shale: dark blue. Other non-net: red.

Development wells are not included in the property evaluation due to limited data acquisition.

3. Interpretation Methods

For the Static Reservoir Model, porosity is calculated from log data and calibrated using stress-corrected core porosity. Permeability is derived from porosity using core-based porosity-permeability relationships at in-situ conditions. Net-to-gross is defined from GR based shale volume and porosity at cut-offs that match density-neutron separations and core observations, whilst the saturation model is based on log derived saturation within the main hydrocarbon-bearing interval, the Captain D.

For overburden and aquifer models, only porosity and net sand can be obtained from the selected well log data. Permeability and capillary pressure entry data were provided by fairway analogue or

regional trends. Pressure gradient and other log data has been used to estimate fluid contacts for the fields within the aquifer model.

3.1. Porosity

The Captain Sandstone interval in the Goldeneye field is well-calibrated because core was obtained from all four exploration wells in the field across subunits A to E. Accordingly, porosity is computed from the density log by calibrating the log curve with the in-situ stress-corrected core plug porosities. This gives a variation in apparent fluid density for use in Equation (1). Details are given below.

Porosity is derived from the following formula:

$$\varphi = \frac{(\rho_{ma} - \rho_b)}{(\rho_{ma} - \rho_{fluid})} \quad (1)$$

Where: ϕ = total porosity (v/v)

ρ_{ma} = matrix (grain) density (g/cm^3)

ρ_b = bulk (FDC) density (g/cm^3)

ρ_{fluid} = fluid density (g/cm^3)

The matrix density is obtained using core grain density derived from routine core analysis reports (Figure 3-1). Core grain density (ρ_{ma}) is not dependant on core porosity for porosities > 10% so it was chosen to derive matrix density by zone.

The derived apparent fluid densities are based on calibrating density log-derived porosity to stress-corrected Helium core-measured porosity. This is based on special core analysis (SCAL) isostatic porosity reduction measurements from 14/29a-3 and 20/4b-6 which give a field ambient-to-in-situ porosity reduction factor (RF) of 0.935 +/- 0.015 at the original effective vertical reservoir stress of 4,675 psia [322 bara].

The resultant porosity (Equation 1) carries an estimated uncertainty of 1 PU in the Goldeneye exploration wells.

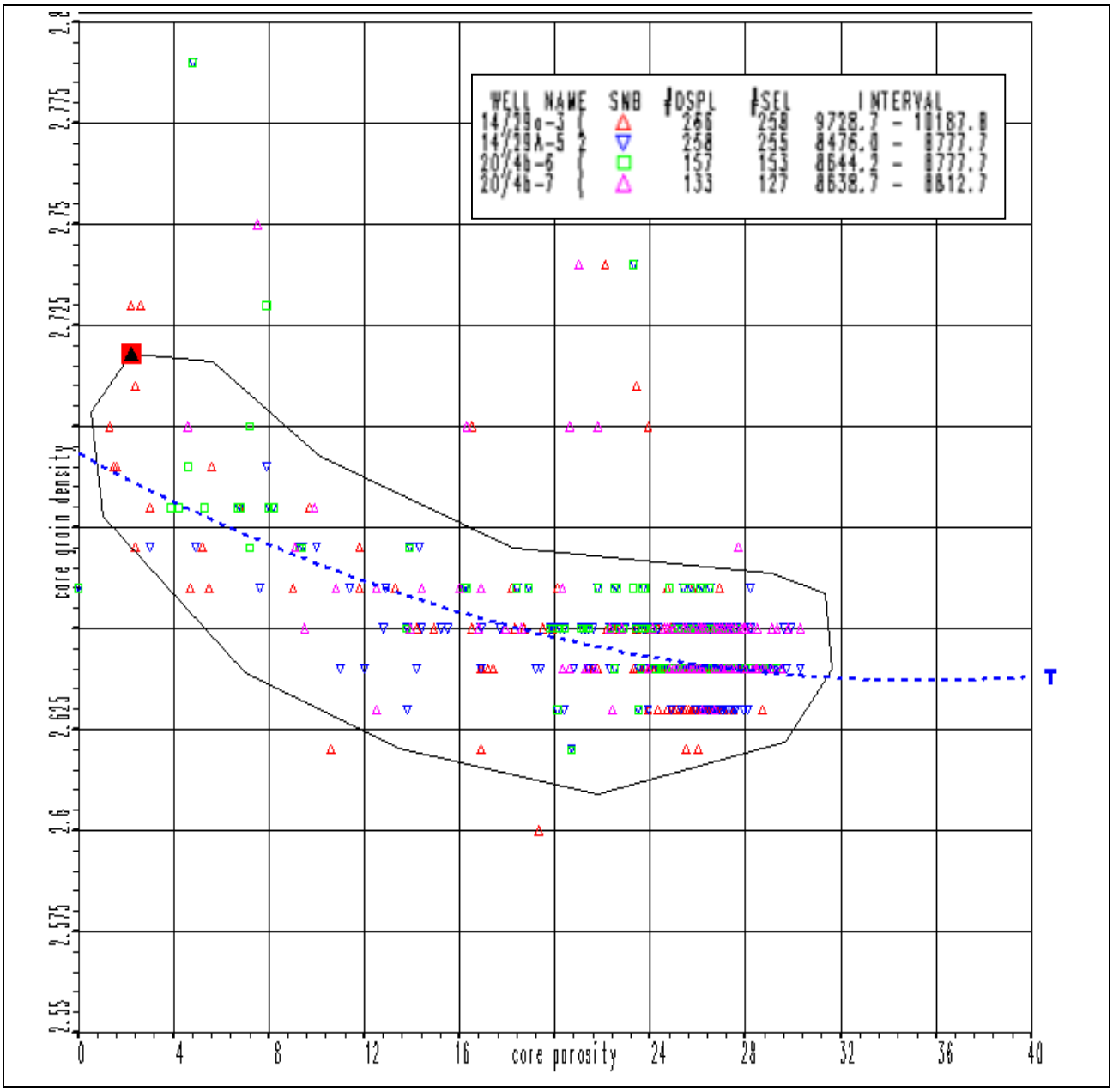

Note: Polygon drawn to exclude extreme data points, trend line is manual to indicate mid-points

Figure 3-1: Core grain density versus core porosity, Goldeneye exploration wells

The zone-dependent matrix density (ρ_{ma}) and fluid density (ρ_{fluid}) are given in Table 3-1 below. For the production wells, where no core was available, an average value was used.

Table 3-1: Matrix and fluid density data, Goldeneye and immediately adjacent exploration and production wells

Well	Fluid zone	Top [ft MD]	Bottom [ft MD]	r_{ma} [g/cm^3]	r_{fluid} [g/cm^3]
14/29a-2	water (Scapa)	8,251	8,387	2.65	1.07
	water (Burns-Sst)	8,392	8,427	2.65	0.9
14/29a-3	gas	9,656	9,676	2.65	0.53
	gas	9,676	9,690	2.65	0.24
	gas	9,690	9,725	2.65	0.15
	gas	9,725	9,832	2.638	0.19
	gas	9,832	9,927	2.638	0.27
	gas	9,927	10,034	2.643	0.53
	oil	10,034	10,064	2.642	0.7
	water	10,064	10,684	2.643	0.8
14/29a-5	gas	8,474	8,648	2.64	0.61
	gas	8,476	8,483	2.64	0.37
	oil	8,648	8,671	2.634	0.72
	water	8,671	9,100	2.634	0.8
20/4b-6	gas	8,616	8,678	2.649	0.83
	oil	8,678	8,700	2.645	0.96
	water	8,700	8,873	2.651	0.96
20/4b-7	gas	8,633	8,646	2.65	0.48
	gas	8,646	8,658	2.651	0.71
	gas	8,649	8,652	2.651	0.5
	oil	8,658	8,679	2.651	0.73
	residual oil + top water leg	8,679	8,722	2.646	0.7
	water	8,722	8,825	2.646	0.76
GYA01-05	gas			2.649	0.22

The apparent fluid densities in the water legs are 0.80, 0.80, and 0.76 g/cm^3 for the OBM wells, and 0.96 g/cm^3 for the WBM well. This shows a consistent picture for the 3 OBM wells, but may be on the low side for the WBM well. One may argue that an apparent fluid density of 1.04 g/cm^3 for the WBM well is more realistic than 0.96 g/cm^3. The 1.04 g/cm^3 value would result in a higher porosity (21.7% versus 20.7%), but would not fit with the current stress correction, the porosity reduction factor of 0.935. As confidence in the Poisson's ratio (0.30) is high – supported by SCAL data - the porosity reduction factor of 0.935, together with the lower apparent fluid density in the water leg, is the preferred interpretation.

The porosity reduction factor at end of field life is extrapolated to be 0.924. There appears to be no clear dependency of porosity reduction factor as function of porosity, facies, or depth. However, there appears to be a larger porosity reduction at lower porosities.

For the development wells, lacking in a full log suite, porosity was derived via a relationship to the GR as determined from the Exploration wells:

$$POR = (-0.15 \times GR + 29.3)/100 \quad (2)$$

For the overburden and aquifer models, the porosity in overburden formations and the Captain fairway is determined using the generic matrix density of 2.65 g/cm^3 for sandstone and 2.71 g/cm^3 for limestone (chalk). Fluid density depends on mud type. Assuming moderate mud filtrate invasion during drilling, the respective values for water-based-mud (WBM) and oil-based-mud (OBM) are 1.1 g/cm^3 and 0.9 g/cm^3. An average porosity reduction factor of 0.96 was used. The reason for using a different reduction factor is that the Poisson's ratio has not been measured on core in the neighbouring wells, and that the porosity reduction in Atlantic is approximately 0.96 if using a Poisson's ratio of 0.30 (14/26a-7a well report).

3.2. Permeability

Core permeability data in the Goldeneye field shows a strong relationship to facies which were built based on geological understanding. For the static field model input, three classes were applied to the Goldeneye exploration wells, each allowing the derivation of permeability from porosity using a different regression (Figure 3-2). The classes were assigned by hand to capture the major groupings of common rock types.

- Class 1. Clean sandstones, predominantly represented in the Captain A and Captain D subunits in their entirety. A prominent medial sand in the Captain C interval is also assigned to this class.
- Class 2. Bioturbated sands and shaley sands of the Captain E.
- Class 3. Shales and interbedded sand-shale intervals, representing most of the Captain C.

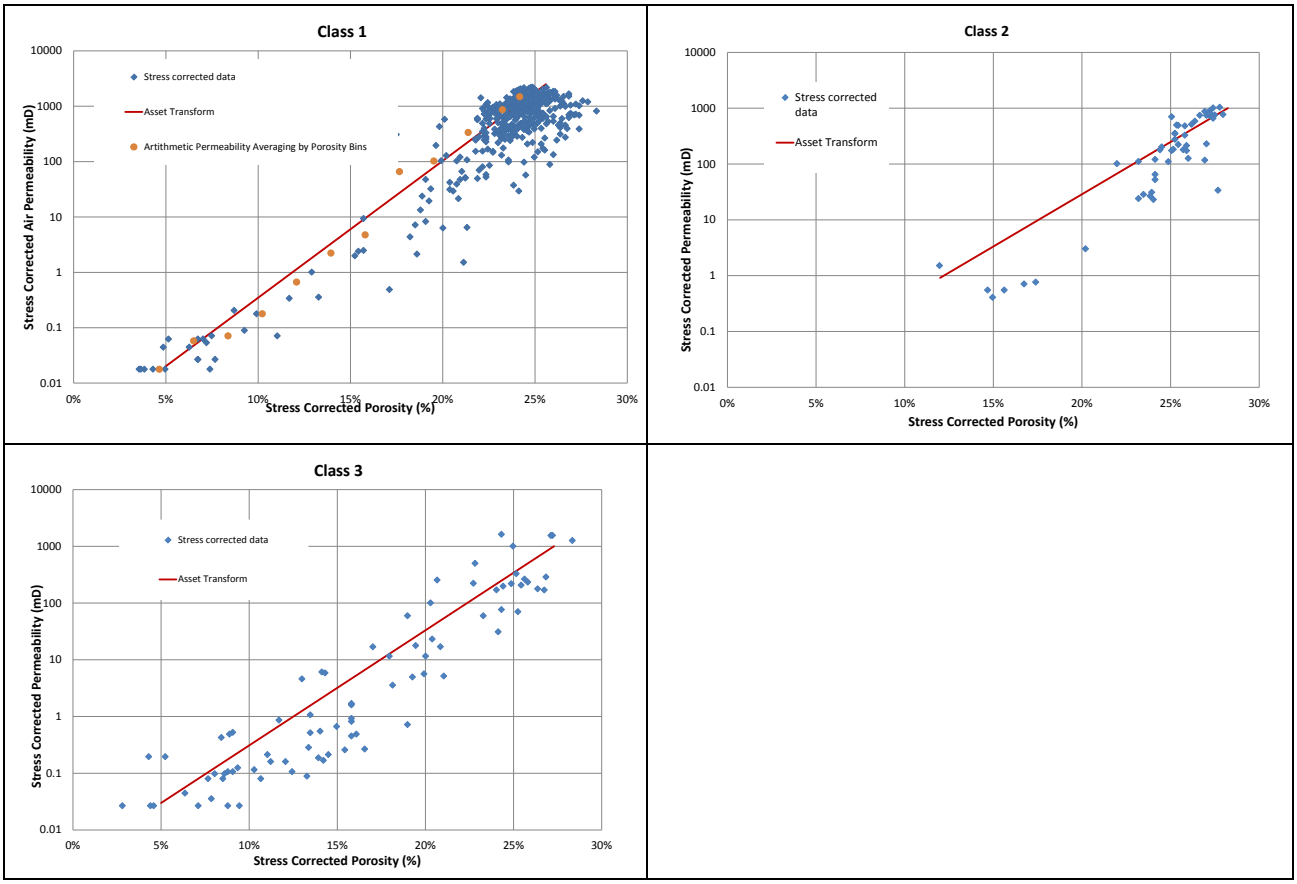

Figure 3-2: Stress-corrected core porosity (% unit – x axis) relationship to stress-corrected core permeability (order of magnitude in mD – y axis) in each facies class

The porosity to permeability relationship for each class is:

$$\begin{aligned} &\text{Class 1 PERM} = \text{MIN}(2500, 10^{(0.2472*(\phi*100)-2.92932)}) \\ &\text{Class 2 PERM} = \text{MIN}(1000, 10^{(0.1873*(\phi*100)-2.28723)}) \\ &\text{Class 3 PERM} = \text{MIN}(2500, 10^{(0.2029*(\phi*100)-2.5382)}) \end{aligned} \quad (3,4,5)$$

Core permeability was corrected to pre-production in-situ properties using permeability under overburden stress measurements from well 14/29a-3 and 20/4b-6. The available measurements were carried out as functions of isostatic stress as follows:

14/29a-3

- Air permeability reduction up to 5,000 psia.
- Brine permeability reduction up to 5,000 psia.

20/4b-6

- No air permeability reduction measurements.

- Brine permeability reduction up to 3,000 psia.

No relation was found between air permeability reduction factors and porosity, permeability, or depth.

- The pre-production air permeability RF is 0.89 (at 3,000 psia [207 bara] isostatic)
- The end of production air permeability RF is 0.86 (at 4,400 psia isostatic)

The in-situ porosity-permeability relationships per facies is based on the ambient core poroperm data after applying the 0.935 porosity RF and the 0.89 pre-production air permeability RF. These in-situ poroperm relationships were applied to the in-situ porosity log to derive continuous in-situ air permeability profiles.

For brine permeabilities, there is a dependency of the brine permeability RF on permeability as expressed in the relationship to air permeability. For air permeabilities above 300 mD the brine-to-air ratio is approximately 0.85. The ratio drops to approximately 0.2 at low permeabilities.

The ratio of in-situ brine permeability (approximated at 3,000 psia isostatic) to air permeability at 400psia is given by:

$$K_{brine,\ in\text{-}situ} / K_{air,ambient} = 0.05 + 0.71 * Exp[-45 / K_{air,ambient}] \quad (6)$$

At end of the production phase, the ratio of in-situ brine permeability at 4,400 psia isostatic to air permeability at 400 psia is estimated to be approximately 0.59.

For the five Goldeneye development wells, which have limited wireline log data, permeability is derived from the deep resistivity log using a relationship developed from the exploration wells. The permeability equation for individual wells is as follows (7):

$$\text{Development Wells Permeability (K)} = (10\text{^}(1.08+1.23*LOG(RES\_DEP)-0.00324*HAFWL))*0.5245 \quad (7)$$

For non-Captain reservoir (Scapa & Burns sandstones), in-situ permeability is derived as follows:

$$\text{Permeability (K)} = MIN(1000,10\text{^}(0.2029*(\phi*100)-2.69729)) \quad (8)$$

Where: K = Permeability (mD)

ϕ = Total Porosity (v/v)

RES_DEP = Deep Resistivity (ohm m)

HAFWL = Height Above Free Water Level (ft)

Permeability for the aquifer and overburden datasets is addressed in Section 4, Analogues.

3.3. Permeability Reconciliation with dynamic data

The static permeability estimates were used during the field development and early CCS planning phases to achieve satisfactory history matches in the dynamic realm. However, recent Goldeneye dynamic history data and inclusion of information from the neighbouring Hoylake field show there is a need to increase reservoir permeability in Goldeneye by a factor of 1.8 to match re-pressurisation performance. An increase in the Goldeneye permeability requires offset by a reduction in the permeability of the aquifer east of the field to balance water encroachment and achieve a match of water breakthrough in the five Goldeneye production wells. The downscaling of permeability of the eastern analytical aquifer model is corroborated by the regional dynamic aquifer model which suggests lower permeabilities in the eastern aquifer by up to 45% to match pressures in the Rochelle field prior to start of Rochelle production. Given the relative coarseness of the relationship used to derive aquifer permeabilities (see Section 4) this is not unreasonable.

To enable this permeability reconciliation, alternative implementations of the porosity-permeability transform were employed. The original static permeabilities were derived from porosity using a geometric relationship. The alternative arithmetic relationship, although apparently overestimating permeability when viewed on a log-linear plot, is known in many fields to give a better match with well test data and in general uplifts derived permeabilities. This was used for Goldeneye and supported the implementation of a permeability multiplier in the dynamic models. The new K/Phi relationship represents an increase in the permeability of 45% compared to the old poro-perm transform (Figure 3-3), with an uncertainty band of 130% to 160% around the old case.

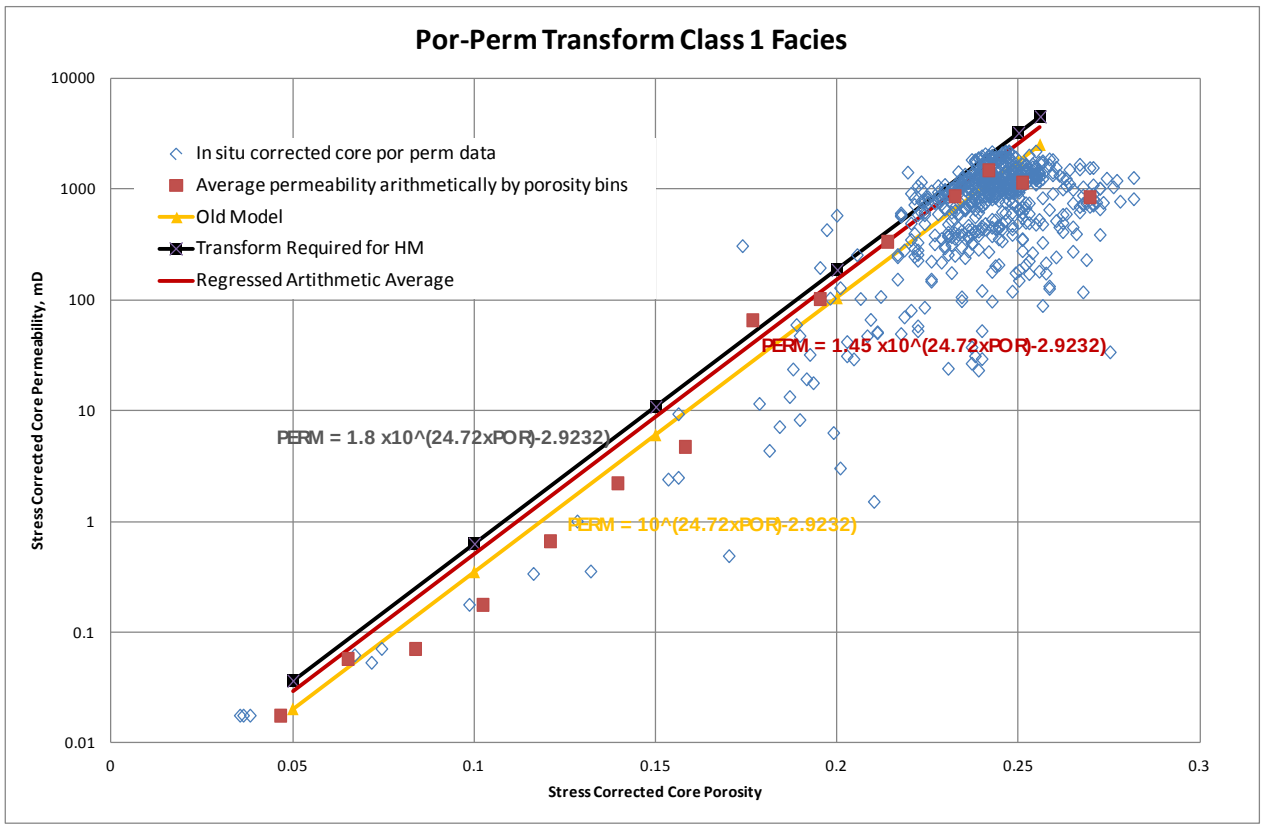

Figure 3-3: Alternative porosity-permeability relationships

The corresponding model permeabilities at well locations were found to be in line with the well test permeabilities derived for three flank wells, GYA5, 20/4b-6 and 20/29a-3, Table 3-2. Other wells

were not addressed as they lay in areas of varying reservoir thickness that would influence the permeability calculation.

Table 3-2: Well test – static permeability comparison, Goldeneye flank wells

	Model K before correction (mD)	Model K after correction	Well Test K	Percentage difference after correction
GYA05	1007	1460	1430	2%
20/4B-6	351	508	553	-9%
20/29A-3	760	1102	1200	-9%

The required additional uplift to match dynamic performance can be found in alternative mechanisms for distributing permeabilities away from the wellbore in the static model. Sequential Gaussian Simulation (SGS) was employed for the production and early CCS work: The SGS methodology can produce significant lateral permeability changes from grid block to grid block in the model, thereby degrading permeability by 5-15% compared to a more uniform layered permeability system. To compensate for this effect the permeability in the FFM would need to be corrected by applying a multiplication factor to the model perms.

Modifications to the two factors porosity-permeability transform and assignment of permeability in the static model enable permeability reconciliation between the static and dynamic realm. The dynamic data shows that in order to match recent re-pressurisation one would need to apply the upper end of the correction band, 1.6 x 1.15 = 1.84.

3.4. Net-to-gross (NTG)

Net-to-gross for the Captain sandstone of the Static Reservoir Model is obtained from the GR derived shale volume and porosity. The porosity cut-off removes tight sandstone streaks which exist mainly in facies class 2.

The GR derived shale volumes are calculated using the following methods:

$$V_{shale} = \frac{GR - GR_{sand}}{GR_{shale} - GR_{sand}} \quad (9)$$

Where: V_{shale} = shale volume (v/v)
GR = measured gamma ray (API)
GR_{sand} = sand baseline gamma ray (API)
GR_{shale} = shale baseline gamma ray (API)

Table 3-3: Sand and shale baselines for shale volume method

Well	Unit	Top [ft MD]	Bottom [ft MD]	GRsand	GRshale
14/29a-2	Scapa	8,251	8,387	35	150
	Burns Sst	8,392	8,427	35	150
14/29a-3	Captain	9,656	10,684	30	80
14/29a-5	Captain	8,474	9,100	25	115
20/4b-6	Captain	8,616	8,845	40	95
20/4b-7	Captain	8,633	8,825	20	80

The resultant shale volume is consistent with the shale volume that is derived from N-D and from core observations.

Based on observations from the four Goldeneye exploration wells, the relevant cut-off for Captain shale volume and porosity is 0.5 and 0.14 respectively, preventing net reservoir appearing in shale sections and giving a good match with cemented layers in core. The impact of varying the V_{sh} cut-off on Equivalent Hydrocarbon Column (EHC) is shown on Figure 3-4 where it can be seen that at V_{sh} of 0.5 over 95% of the EHC is captured. Therefore net-to-gross in the Captain sands is defined by the following conditions:

- Shale volume $V_{shale} < 0.5$
- $\phi > 0.14$

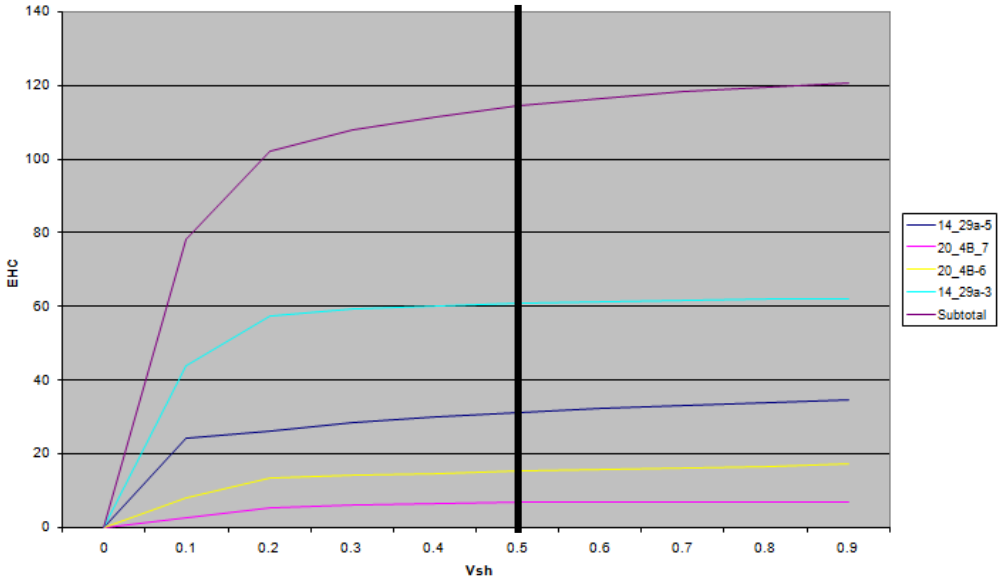

Figure 3-4: Effect of Vsh cut-off on Equivalent Hydrocarbon Column EHC

Overburden formations and the Captain sandstones in the Captain fairway use normalised GR logs and common baselines, with shale volume cut-off as above. The porosity cut-off is set to 0.1. The

exception is the upper chalk group, which based on log readings, has clean properties throughout the Ekofisk, Tor and Hod yielding a net-to-gross ratio of 1.

3.5. Fluid Contacts and Free Fluid-Level

Three fluid phases (gas, oil and water) are present in the Goldeneye Captain sands. Fluid levels are obtained from open-hole pressure data, whilst fluid contacts are obtained using core and logs to cross check the fluid level reading (Table 3-4). Original Goldeneye field pressure data is derived from Wells 14/29a-3, 14/29a-5, 20/4b-6 and 20/4b-7, plotted in Figure 3-5. The 14/29a-3 data is slightly offset from the common hydrocarbon gradient due to different tool calibration and greater measurement depth uncertainty.

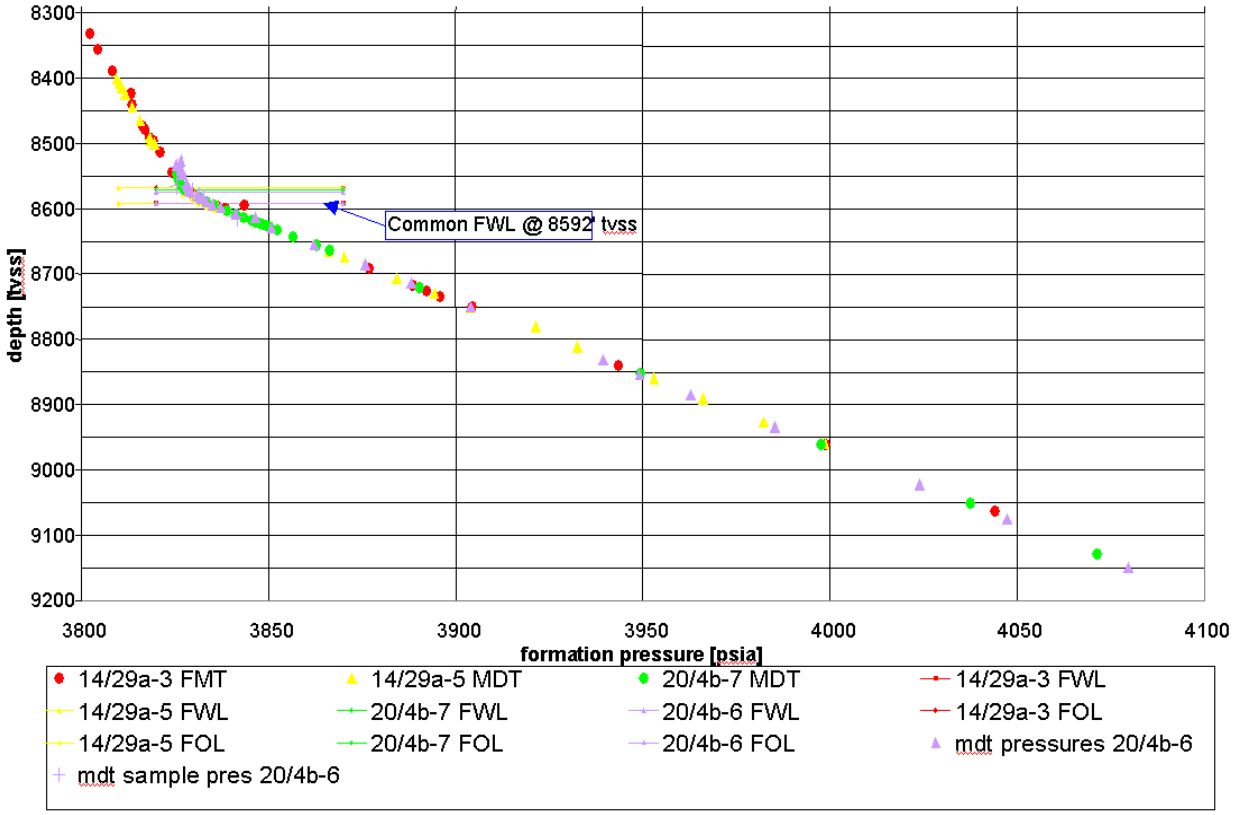

Figure 3-5: **Goldeneye pressure data in the Captain Sandstone, depths in feet. The intersection of hydrocarbon and water gradients indicates the FWL**

Table 3-4: **Summary of fluid distribution data for Goldeneye Exploration Wells**

Well	Source	GUT	GDT	GOC	OUT	FOL	OWC	FWL
14/29a-3	**Log**	8265	8547	N/L	8570		8590	
	MDT					8567		8592
	Core	N/L.	8547	N/L	8569		8588	
14/29a-5	**Log**	8393	8498	N/L	8567		8589	
	MDT					8564		8588
	Core	8394	8498	N/L	8566		8593.5	
20/4b-6	**Log**	8523	N/A	8571	N/A		8591	

	MDT					8575	8593
	Core	N/L	N/A	8570	N/A	8592	
20/4b-7	**Log**	8546.5	N/A	8567.5	N/A	8593.5	
	MDT					8572	8593
	Core	N/L	N/A	8569.5	N/A	8595	

Note: Units are ft TVDSS. GUT= gas up to; GDT = gas down to, GOC = gas-oil contact, OUT = oil up to, FOL = free oil level, OWC = oil-water contact, FWL = free water level, N/L = Not Logged.

The main conclusions are set out below.

The aquifer pressure data between all four Goldeneye wells line up on a water gradient of 0.4408 psi/ft. The Goldeneye Reservoir in-situ gas gradient is 0.097 psi/ft. The oil gradients cannot be determined accurately due to the small vertical extent of the oil column: the calculated gradients vary from 0.295 psi/ft, to 0.35 psi/ft.

A free water level (FWL) of 8,592 ft to 8,593 ft [2,618.84 m to 2,619.15 m] TVSS are measured in the Goldeneye Reservoir. The shallower FWL 8,592ft TVSS is taken as the common Goldeneye FWL. An oil rim thickness of 24-25 ft is found in wells 14/29a-3 and 5; the oil rim thickness is 21 ft in wells 20/4b-6 and 7. This implies a discontinuity or seal in the oil rim between the 14/29a wells where the contacts are in the laterally variable Captain C and the 20/4b wells where the contacts are in the more continuous Captain D.

In general a good agreement is found between the different methods to pick the gas/oil and oil/water fluid interfaces, with a maximum difference of 2 ft between the FWL and oil water contact (OWC) (FWL & OWC are several feet shallower for well 14/29a-5, possibly due to problems with depth control). The field-wide Free Water Level is picked at 8,592 ft TVDSS and the free oil levels at 8,567 ft TVDSS for the northern half of the field, 8,575 ft TVDSS for the southern half.

The Goldeneye overburden formations are relevant for containment and secondary storage modelling: they are water bearing. There is no indication of hydrocarbon based on log data, cuttings and gas chromatograph readings. The only possibility of hydrocarbon content comes from shallow gas in the Tertiary Skade Formation of the Westray Group, approximately 1,500 ft [457 m] TVDSS, some 6,700 ft above top Captain, which shows 1-3% total gas based on gas chromatograph interpretation in several development wells. Shallow gas at this and shallower levels is widely reported across the Outer Moray Firth and Wytch Ground Graben (e.g. Holmes & Stoker 2005 (2)) and is not attributed to leakage from underlying reservoirs.

To be able to differentiate between properties in hydrocarbon and water legs separately for aquifer modelling, the pressure and FWL in fields within the Captain fairway is examined locally. These are stated below from east to west (see Figure 2-2 for locations).

- **Hannay**

  The hydrocarbon well is 20/5c-6, containing an oil column. Other wells surrounding the field, 14/30b-3 and 14/28b-2, are included to provide analysis for the regional water gradient.

- **Hoylake**

  Interpreted wells are 14/29a-4 and 20/4b-3, where only 14/29a-4 contains a gas column. These exploration wells were plugged and abandoned.

- **Atlantic**

  Interpreted wells are 14/26a-6, 14/26a-8, 14/26-1 and 14/26a-7a, all of which have gas columns on the top of the water leg.

- **Cromarty**

  One well contains a gas column, 13/30-3. Several wells are also included, 13/30-1, 13/30-2 and 13/30a-4, to observe the regional water gradient.

- **Blake**

  The furthest field to the west of the evaluation scope, one water-wet well is included, 13/24-1.

Water gradients across the fields from pre-production pressure data suggest common aquifer flow across the Captain fairway as seen in Figure 3-6. Fluid contacts for individual wells in the main fields are listed in Table 3-5.

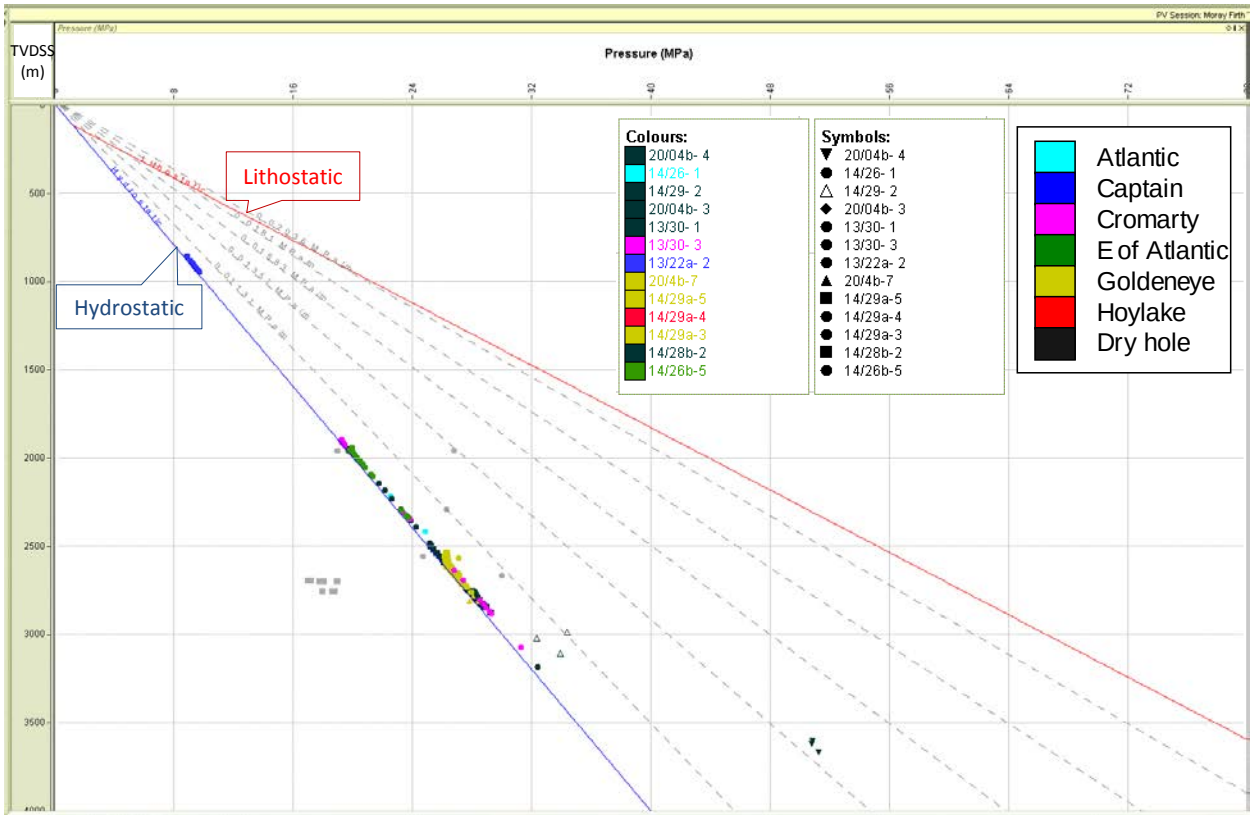

Note: Light grey data are suspect pressures

Figure 3-6: Uniform water pressure gradient in the fields within the Captain fairway

Table 3-5: Fluid contacts in selected wells surrounding Goldeneye

*Well	14/29a-4	20/5c-6	14/26a-6	14/26a-8	14/26-1	13/26a-7a	13/30-3
Location	Hannay	Hoylake	Atlantic	Atlantic	Atlantic	Atlantic	Cromarty
Gas or oil water contact (ft TVDSS)	9,505	8,795	6,447	6,471	6,443	6,463	6,245

The Atlantic GOC is taken by the operator at 6,470 ft TVDSS, OWC at 6,474 ft TVDSS on the basis of pressure data.

3.6. Saturation height model

The Goldeneye saturation height model is derived using the Leverett-J (3) method on logging data to derive a Saturation-Height Function (SHF). The log input only includes clean sand which satisfies the following criteria:

- Porosity above 20%
- Low clay content, CEC < 0.1 meq/ml

Unit D, the main CO_2 container, presents a massive and continuous sand across Goldeneye. It is thoroughly uniform and clean with a low clay content, satisfying the above criteria.

The initial saturation model is calculated from clean sand logging data. It is then compared with normal log derived saturations and saturation-height curves derived from mercury injection capillary pressure data. Water saturations produced from these inputs show good agreement, with uncertainty less than 0.05s.u. within net intervals.

In Goldeneye, resistivity logs have been calibrated in clean water bearing sands on a well-by-well basis meaning that the Archie method (4) is well suited for log saturation evaluation. Accordingly, the Archie log saturation is calculated to verify the Leverett-J model performance using water resistivity from a Pickett Plot and Archie parameters (saturation and cementation exponent) from wells 14/29a-3 and 20/4a-6. The comparison is shown in Figure 3-7.

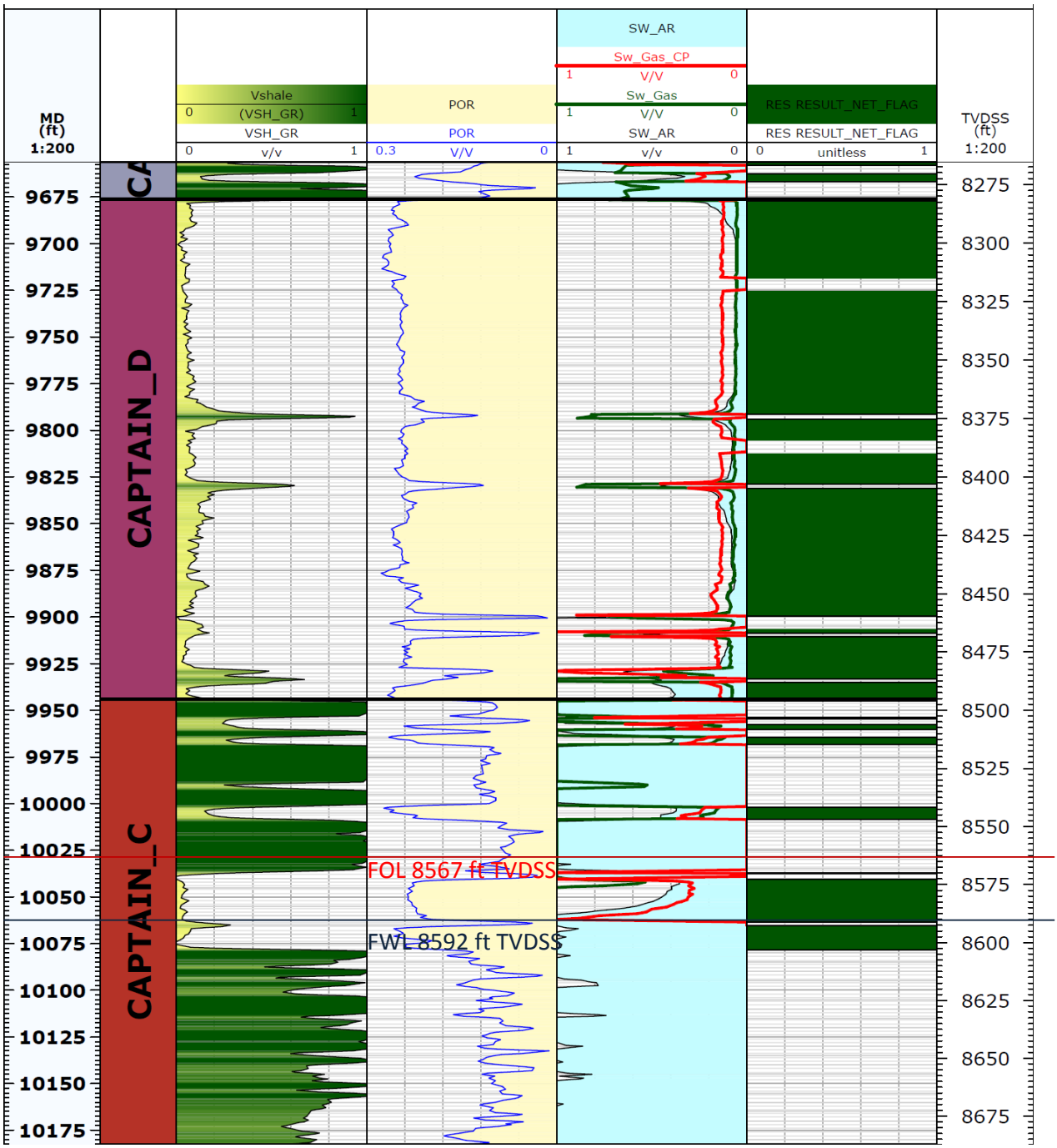

Figure 3-7: Saturation height derived Sw comparison to Archie log saturation in well 14/29a-3.

Note: Black curve is Archie Log saturation, Green curve is Log SHF derived Sw and Red is Capillary Pressure SHF derived Sw. Note that green curve terminates at GOC – represents 1-Sg rather than true Sw.

Log data from wells 14/29-a3 and 20/4b-6 are used as input to the Leverett-J method producing two saturation models, for gas and oil. The additional inputs are fluid gradients from the pressure plot, minimum saturation from log at infinite HAFWL, and default reservoir interfacial tension based on hydrocarbon content.

The input detail is listed in Table 3-6 for gas saturation and Table 3-7 for oil saturation. The equation is as follows:

$$J = \frac{HAFWL}{\sigma \cdot \cos\theta} \cdot \sqrt{\frac{K}{\phi}} \cdot (\rho_{water} - \rho_{hc}) \quad (10)$$

Where: J = Leverett-J function (unitless)
HAFWL= height above free water level (ft)
σ = interfacial tension (mN/m)
θ = contact angle (deg)
K = permeability (mD)
ϕ = total porosity (v/v)
ρ_{water} = water density gradient (psi/ft)
ρ_{hc} = hydrocarbon density gradient (psi/ft)

Table 3-6: Gas reservoir parameter input

Parameter		14/29a-3	20/4b-6	Field
FWL	*[ft TVDSS]*	8,590.9	8,592	8,592
σ	*[mN/m]*	31	31	31
ρ_{water}	*[psi/ft]*	0.44	0.44	0.44
ρ_{gas}	*[psi/ft]*	0.103	0.103	0.103
θ_{gw}	*[deg]*	0	0	0
$S_{w\text{-}irr}$	*[frac]*	0.02	0.02	0.02

Table 3-7: Oil reservoir parameter input

Parameter		14/29a-3	20/4b-6	Field
FWL	*[ft TVDSS]*	8,590.9	8,592	8,592
σ	*[mN/m]*	25	25	25
ρ_{water}	*[psi/ft]*	0.44	0.44	0.44
ρ_{oil}	*[psi/ft]*	0.32	0.30	0.32
θ_{ow}	*[deg]*	50	50	50
$S_{w\text{-}irr}$	*[frac]*	0.02	0.02	0.02

4. Analogues

Limited permeability and capillary pressure entry in the overburden and some wells in the Captain fairway drives the need to use representative analogue data for the overburden and aquifer static models. The bullets below describe each requirement for analogue data and the appropriate analogue used in the models.

- **Permeability analogue for the Chalk Group:**

  The Chalk Group is water bearing and based on current investigation, does not contain any geological feature which may suggest reservoir property enhancement. However, it does not guarantee that fine fracture networks do not exist. The analogue data is provided by a Shell internal chalk study for the North Sea UK Sector under the current working assumption that the chalk is in matrix condition. The study incorporates plug measurements from the Ekofisk, Tor and Hod formations and the result is applied additionally to the Herring Formation due to the uniformity observed from the logs. The results indicate that brine permeability for these formations of the Chalk Group can be set at 0.001 mD. This is used in the overburden model.

- **Capillary entry pressure analogue for the Chalk Group:**

  Capillary entry pressure is derived from Poisson's ratio and porosity using the method described in a paper on Danish Chalk (5). The paper states that Poisson's ratio is related to carbonate content and pore stiffness; therefore it sufficiently reflects surface area which correlates to capillary entry pressure. With the absence of core measurement, Poisson's ratio can be determined from the sonic and shear logs using the following method:

$$\upsilon = (\upsilon_P^2 - 2\upsilon_S^2)/(2(\upsilon_P^2 - \upsilon_S^2)) \quad (11)$$

  Where: υ = Poisson's ratio

  υ_p = Sonic slowness (ft/s)

  υ_s = Shear slowness (ft/s)

  Shear logs are available from all four Goldeneye exploration wells.

  The relationship between capillary entry pressure, porosity and Poisson's ratio based on observation from several chalk reservoirs in Denmark and the Pierce field chalk in the UK sector is displayed in Figure 4-1. Goldeneye overburden formations have Poisson's ratio between 0.3 and 0.35 which is similar to Pierce Chalk data. This is used in the overburden model.

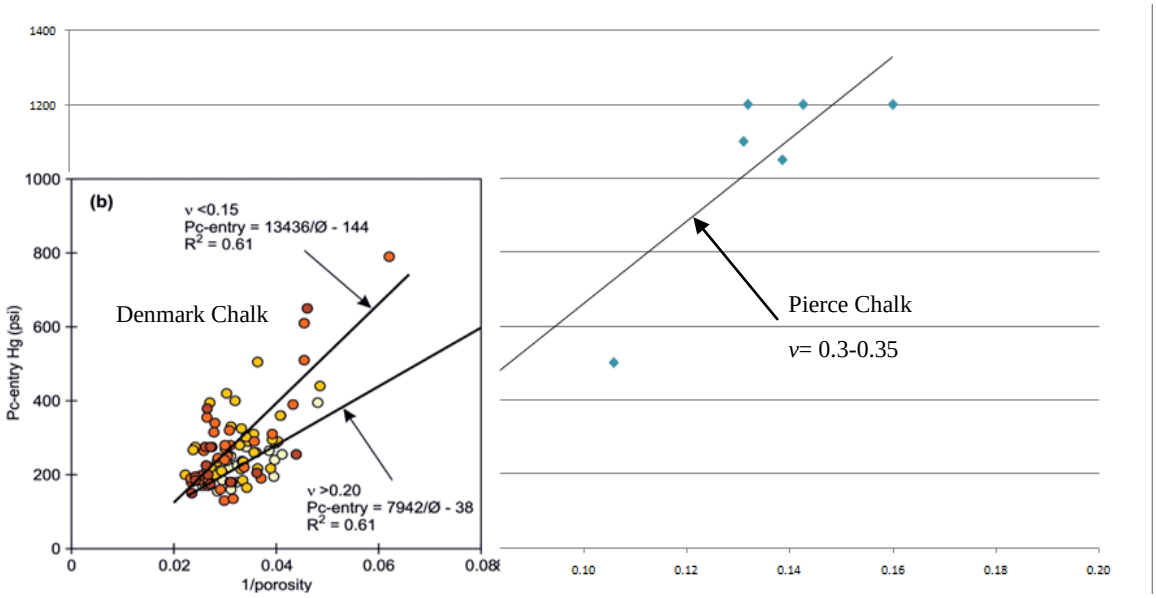

Figure 4-1: Capillary entry pressure prediction using porosity and Poisson's ratio described in Fabricius et al. 2007

- **Permeability analogue for Goldeneye Montrose Group:**

  The three main sandstone intervals of the Montrose Group are addressed separately, in each case using analogue field and well data to derive porosity-permeability transforms to allow permeability derivation from log porosity. For the Balmoral sandstones the analogous Flyndre field (6) provided relevant data. Two transforms were used, one for clean sands (Vsh <10%) and one for shaley sands (Vsh between 10-50% where the Vsh cut-off for net sand was 50%).

  For the Mey sandstones poroperm data were compared from published values for the Blenheim field (7) 80 km northeast of Goldeneye and from the laterally equivalent Andrew sandstone in well 14/26b-4, 50 km northwest of Goldeneye and 3 km north of Atlantic.

  For the Maureen Sandstones, data was assembled from the Everest complex of fields, 130 km east of Goldeneye (8). Two rock types were recognised with distinct porosity characteristics driven by diagenesis – the porosity classes could be replicated in Goldeneye and accordingly two relationships were applied.

- **Permeability analogue for fairway Captain fairway sandstone (excluding Goldeneye):**

  Several wells in the Captain fairway have core acquired from within the Captain sandstone, and for most fields the permeability could be defined using a porosity transform for each field. An example is the Atlantic field shown in Figure 4-2.

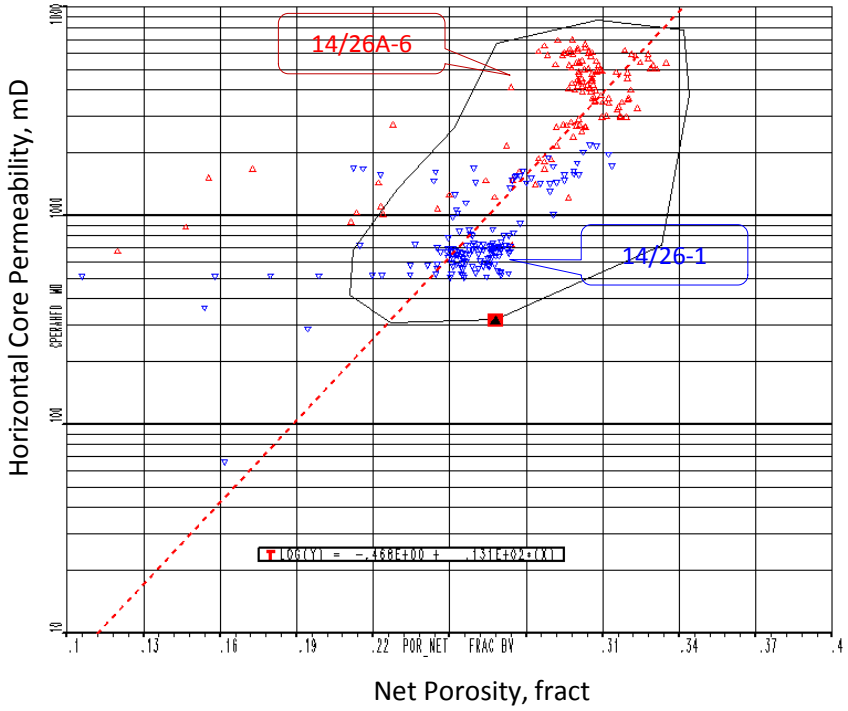

Figure 4-2: Porosity to permeability relationship used to determine permeability in the Captain Sst within the Atlantic field. Regression given as red line.

For small fields or exploration wells drilled between fields, permeability is calculated using a regional permeability relationship averaging the data from the fields along the fairway.

$$k\_phi = 0.601 \times 10^{11.5 \times \Phi} \quad (12)$$

Where: k_phi = Permeability (mD)

ϕ = Total Porosity (v/v)

Using this relationship provides a rough estimate of permeability along the Captain fairway. However, for very high porosities (greater than 32%) the equation extrapolates to unreasonably high permeabilities (3+ Darcies). Thus, the permeability curve was clipped at a maximum of 2,500 mD (which corresponds to a maximum porosity of 0.3147).

This permeability data is used in the aquifer model.

5. Input to Static and Dynamic Model

Three reservoir models have been built to simulate the Goldeneye Captain reservoir performance and model CO_2 behaviour. Porosity, Permeability, NTG and fluid contacts are the inputs to all static models and then upscaled for input to the dynamic Full Field Model (FFM) with the addition of saturation height functions. The detail of the property input to the static model suite is included in the Static Model Report. Input properties for the overburden and aquifer static models are stated in Table 5-1 and Table 5-2 respectively.

Table 5-1: Property input to overburden static model by formation

Formation	Ave Por (v/v)	Ave net to gross	Ave Perm (mD)
Moray Gp	0.326	0.468	470
U Dornoch Sst Unit	0.34	0.47	370
Dornoch Mudstone Unit	0.34	0.27	80
L Dornoch Sst Unit	0.31	0.39	290
Montrose Gp (Lista Shale)	0.242	0.06	0
Mey Sst Mb	0.34	0.46	210
U Balmoral Sst Unit	0.30	0.61	350
L Balmoral Sst and Tuffite Unit	0.27	0.81	350
Maureen Fm	0.24	0.83	370
Ekofisk Fm.	0.11	1.00	0.001
Tor Fm	0.04	1.00	0.001
Hod Fm	0.06	1.00	0.001
Herring Fm	0.05	0.99	0.001
Plenus Marl Fm	0.07	0.40	0
Hidra Fm	0.05	0.99	0

Note: Group (Gp), Upper (U), Lower (L)

Input from 9 wells, see Table 2-1.

Table 5-2: Property input to aquifer model based on wells

Field	Well	Ave Por (v/v)	Ave net to gross	Ave Perm (mD)
Blake	13/24-1	0.319	0.197	110
Water wells	13/30-1	0.231	0.740	852
Water wells	13/30-2	0.277	0.759	1285
Cromarty	13/30-3	0.313	0.890	1865
Water wells	13/30a-4	0.274	0.715	934
Atlantic	14/26-1	0.277	0.730	694
Atlantic	14/26a-6	0.317	0.821	1468
Atlantic	14/26a-7A	0.306	0.529	1795
Atlantic	14/26a-8	0.340	0.840	1583

Field	Well	Ave Por (v/v)	Ave net to gross	Ave Perm (mD)
West of Goldeneye	14/28b-2	0.234	0.768	1022
Goldeneye	14/29a-3	0.288	0.757	700
Goldeneye	14/29a-5	0.201	0.482	700
Goldeneye	20/4b-6	0.240	0.783	700
Goldeneye	20/4b-7	0.276	0.705	700
East of Goldeneye	14/30b-3	0.232	0.700	279
Hoylake	14/29a-4	0.239	0.672	510
Hoylake	20/4b-3	0.228	0.880	406
Hannay	20/5c-6	0.232	0.663	331

These overburden and aquifer properties may be varied to reflect sensitivities in dynamic modelling during fluid migration scenario simulation.

6. References – Bibliography

1. PCCS-05-PTD-ZG-0580-00001, Static Model Reports, Key Knowledge Deliverable 11.108.
2. Holmes, R & Stoker, S.J. 2005. Investigation of the origin of shallow gas in Outer Moray Firth open blocks 15/20c and 15/25d. BGS Report to Dept of Trade and Industry No. GC04/22.
3. M.C. Leverett (1941). "Capillary behaviour in porous solids". *Transactions of the AIME* (142): 159–172
4. G.E. Archie, The Electrical Resistivity Log as an Aid in Determining Some Reservoir Characteristics, Dallas Meeting, October 1941
5. Fabricius et al. (2007) How depositional texture and diagenesis control petrophysical and elastic properties of samples from five North Sea chalk fields. Petroleum Geoscience 13, 81-95.
6. Engstrøm, F. et al (2010) Flyndre Field - tilted oil water contact in a thin Palaeocene sandstone reservoir. Presentation pack for DEVEX 2010.
7. Dickinson et al (2001). Blenheim field: the appraisal of a small oilfield with a horizontal well. Petroleum Geoscience, 7, 81-95.
8. O'Connor, S.J. & Walker, D. (1993). Palaeocene reservoirs of the Everest trend. In: (J.R. Parker, ed) Petroleum Geology of North-West Europe: Proceedings of the 4th Conference. The Geological Society, London, 145-160.

7. Glossary of Terms

Term	Definition
BGS	British Geological Survey
CCGT	Combined cycle gas turbine
CCS	Carbon Capture and Storage
CEC	Cation Exchange Capacity
CO_2	Carbon Dioxide
EHC	Equivalent Hydrocarbon Column
FDC	Formation Density Compensated
FFM	Full Field Model
Fm	Formation
FOL	Free Oil Level
FWL	Free Water Level
GDT	Gas down to
GOC	Gas Oil Contact
GOC	Gas-oil contact
GR	Gamma Ray
GR NORM	Normalized Gamma Ray
GUT	Gas up to
HAFWL	Height Above Free Water Level
IFT	Interfacial Tension
LWD	Logging While Drilling
Mb	Member
MCT	Mechanical Coring Tool
MD	Measured Depth
MDT	Modular Dynamic Tester*
N/L	Not Logged
NTG	Net to Gross
OBM	Oil Based Mud
OUT	Oil up to
OWC	Oil Water Contact
PU	Porosity Unit
RF	Reduction factor
RF	Porosity Reduction Factor
RFT	Repeat Formation Tester
s.u.	Saturation Units – units of the property measured.
SCAL	Special Core Analysis
SGS	Sequential Gaussian Simulation
SHF	Saturation-Height Function
Sst	Sandstone
Sw	Water Saturation
TVDSS	True vertical depth sub-sea
WBM	Water Based Mud

In the text, well names have been abbreviated to their operational form. The full well names are given in Table 7-1 below.

Table 7-1: Well name abbreviations

Full well name	Abbreviated well name
DTI 14/29a-A3	GYA01
DTI 14/29a-A4Z	GYA02S1
DTI 14/29a-A4	GYA02
DTI 14/29a-A5	GYA03
DTI 14/29a-A1	GYA04
DTI 14/29a-A2	GYA05

8. Glossary of Unit Conversions

Table 8-1: Unit Conversion Table

Function	Unit - Imperial to Metric conversion Factor
Length	1 Foot = 0.3048 metres
Pressure	1 bara = 14.5 psia

APPENDIX 1. Permeability facies-class depths

Table 8-2: Permeability facies-class depths

Well	Top (ft md)	Base (ft md)	Facies Classes
14/29a-3	9656	9676	2
14/29a-3	9676	9944.5	1
14/29a-3	9944.5	10037	3
14/29a-3	10037	10078	1
14/29a-3	10078	10100.5	3
14/29a-3	10100.5	10132	Non-Net
14/29a-3	10132	10183	3
14/29a-3	10183	10684	1
14/29a-5	8475	8499.5	2
14/29a-5	8499.5	8569.5	1
14/29a-5	8569.5	8649	3
14/29a-5	8649	8677.5	1
14/29a-5	8677.5	8740	Non-Net
14/29a-5	8740	8784	3
14/29a-5	8784	8895.5	1
14/29a-5	8895.5	8956	3
14/29a-5	8956	9043.5	1
14/29a-5	9043.5	9100.5	3
20/4b-6	8615	8637.5	2
20/4b-6	8637.5	8777.5	1
20/4b-6	8777.5	8794	3
20/4b-6	8794	8809	1
20/4b-6	8809	8826	3
20/4b-6	8826	8845	1
20/4b-6	8845	8910.5	Non-Net
20/4b-6	8910.5	9371.5	Non-Net
20/4b-7	8632.5	8668.5	2
20/4b-7	8668.5	8759	1

20/4b-7	8759	8803	3
20/4b-7	8803	8824	1
20/4b-7	8824	8880	Non-Net
20/4b-7	8880	9372	Non-Net